



Low-field magnetoresistance of $\text{La}_{0.7}\text{Ca}_{0.3}\text{MnO}_3$ perovskite synthesized by reactive milling method

D.H. Manh^{a,*}, P.T. Phong^b, T.D. Thanh^a, L.V. Hong^a, N.X. Phuc^a

^a Institute of Materials Science, Vietnam Academy of Science and Technology, 18 Hoang Quoc Viet Road, Cau Giay Distr., Hanoi, Viet Nam

^b Nha Trang Pedagogic College, 1 Nguyen Chanh St., Khanh Hoa Province, Viet Nam

ARTICLE INFO

Article history:

Received 4 January 2010
Received in revised form 18 March 2010
Accepted 21 March 2010
Available online 27 March 2010

Keywords:

Manganite
Low-field magnetoresistance
Grain size
Spin-polarized tunneling

ABSTRACT

Nanocrystalline, granular samples of $\text{La}_{0.7}\text{Ca}_{0.3}\text{MnO}_3$ (LCMO) were synthesized by reactive milling method and annealed at various temperatures. Effect of grain size on the low-field magnetoresistance (LFMR) has been investigated. Based upon a phenomenological model taking into account the spin-polarized transport across grain boundaries, we explained magnetic field dependence of magnetoresistance in LCMO samples. The contribution to the magnetoresistance coming from spin-polarized tunneling was separated out from the intergranular contribution. The fitted results showed that the temperature dependence of the LFMR displays a Curie–Weiss law-like behavior.

© 2010 Elsevier B.V. All rights reserved.

1. Introduction

The colossal magnetoresistance (CMR) in manganites with formula $\text{D}_{1-x}\text{A}_x\text{MnO}_3$ (where D is a trivalent rare earth and A is a divalent alkaline earth ion) is obtained around the paramagnetic (PM) to ferromagnetic (FM) transition temperature (T_C) at a high magnetic field, which restricts their applicability on devices. This effect is explained in terms of the double exchange (DE) models [1]. The low-field magnetoresistance (LFMR) was discovered in polycrystalline manganites samples (both bulk and thin films) [2]. The LFMR is due to spin-polarized tunneling between neighbouring grains and is completely absent in single crystals. There are two main ways to increase LFMR: (i) reducing the grain size of the ceramics would imply an increase in the LFMR [3–7] or (ii) creating a second phase into the ferromagnetic manganite matrix had resulted in an enhancement of the LFMR. These secondary phases include, for example, artificial boundary of the insulating oxides [8–10] and polymer composites [11,12].

There are several reports on the influence of grain size to LFMR properties [3,5,13,19–21]. First, Balcells et al. [5] have presented that LFMR of $\text{La}_{0.7}\text{Sr}_{0.3}\text{MnO}_3$ (the samples prepared by the conventional ceramic method with grain size from 0.5 to 100 μm) not only decreases with temperature but also depends on the grain size, becoming smaller as increasing the grain size. Additionally, the temperature dependence of LFMR displays a Curie–Weiss behavior,

i.e. $\text{LFMR}(T) = a + b/(T + c)$, which is characteristic of spin-polarized tunneling in granular ferromagnetic systems [2]. In contradiction with the results of Balcells et al. [5], Siwach et al. [13] observed that LFMR of LCMO (the samples synthesized through the polymeric precursor route with grain size from 25 to 100 nm) increases with grain size and the maximum LFMR obtained with the grain size of 100 nm. Recently, Dey and Nath [3] showed that the LFMR value in LCMO (grain size from 17 to 27 nm) remains constant up to sufficiently high temperature ($\sim 220\text{K}$) and then drops sharply with temperature. These results show that the LFMR–grain size dependence in manganites depends strongly on the different synthesis conditions, as the intergranular disorder plays an important role in determining the LFMR.

In this study, we mainly analyzed the effects of grain size on the LFMR of $\text{La}_{0.7}\text{Ca}_{0.3}\text{MnO}_3$. A phenomenological model of Raychaudhuri et al. [14], based on the spin-polarized transport of conduction electrons across grain boundaries, used to evaluate the magnetic field dependence of magnetoresistance in granular LCMO. We also found that the temperature dependence of the part of the MR coming from spin-polarized tunneling (MR_{SPT}) displays a Curie–Weiss law-like behavior and the fitting parameter c increases monotonically when increasing the grain size.

2. Experimental

$\text{La}_{0.7}\text{Ca}_{0.3}\text{MnO}_3$ (LCMO) nanoparticles were prepared by reactive milling method. La_2O_3 , CaCO_3 and MnO_2 powders with purity 99.9% from Merck were used as the starting materials. Phase-pure completely LCMO powders obtained after 8 h of milling time in the ambient atmosphere [15]. Finally, the resulting powder was pressed into circular pellets and annealed at 600 °C (S1), 650 °C (S2), 700 °C (S3),

* Corresponding author.

E-mail address: manhhdh@ims.vast.ac.vn (D.H. Manh).

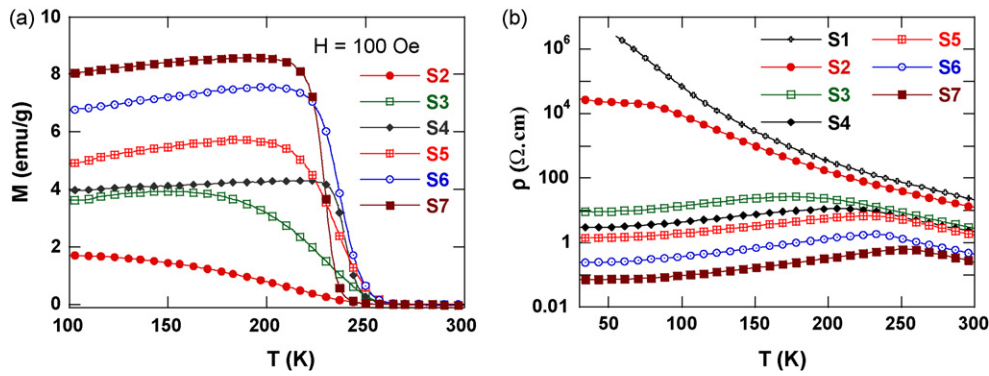


Fig. 1. (a) The size dependence of M - T curves in magnetic field of 100 Oe and (b) temperature dependence of resistivity for LCMO with different particle size.

750 °C (S4), 800 °C (S5), 900 °C (S6) and 1000 °C (S7) for 2 h to obtain different grain size samples.

The DC magnetization measurements were done using a vibrating sample magnetometer (VSM). The dc resistivity measurements have been carried out by standard dc four-probe technique in the temperature range of 30–300 K using a closed cycle helium refrigerator cryostat with Keithley instruments without or with magnetic fields (0–3 kOe). The MR ratio is defined as $MR = [\rho(0, T) - \rho(H, T)] / |\rho(0, T)|$, where $\rho(0, T)$ and $\rho(H, T)$ are the resistivity values for zero and applied fields, respectively.

3. Results and discussions

The room temperature X-ray diffraction (XRD) patterns and the SEM micrographs of the LCMO samples are reported elsewhere [16]. We have already shown that the samples are orthorhombic and of single phase without any detectable secondary phase. The average crystallite size of S3, S4, S5, S6 and S7 samples, deduced from XRD data, is calculated to be ~ 16 nm, 21 nm, 35 nm, 43 nm and 73 nm, respectively. In this report, the grain/particle size will hereafter be referred to as the crystallite size.

Fig. 1(a) shows the temperature dependence of magnetization in magnetic field of 100 Oe for LCMO. We can see that the magnetization decreases as the grain size diminishes whereas the ordering temperature T_C only changes minimally. A similar feature can also be seen in a measurement of the size dependence of high-field M - T curves ($H = 5$ kOe) for the same samples [16]. Up to now, a model of the particles in which the inner part could have the same magnetic property as the bulk compound, but the outer layer would contain a magnetically disordered state is conceded widely to explain the size dependence of magnetization [3,7,16]. On the other hand, the magnetization is reduced because the influence of the outer layer increases as the particle size decreases. Surface contribution is larger for smaller particles and therefore the magnetization is diminished in a proportional way.

The temperature dependence of resistivity was measured by the four-probe method between 30 and 300 K. As plotted in Fig. 1(b) the resistivity of the LCMO samples exhibit strong dependence on the annealing temperature and hence the grain size. For all the samples the resistivity decreases as the grain size increases. The grain size increases leading to a decrease in the grain boundaries and the associated disorder. This results in a decrease in scattering of the carriers expressed by a decrease in the resistivity. The characteristic insulator-metal transition temperature T_{MI} is measured to be ~ 175 K, ~ 207 K, ~ 226 K, ~ 230 K and ~ 250 K for samples S3, S4, S5, S6 and S7, respectively. We almost have not observed the T_{MI} for the samples annealed at 600 °C (S1) and 650 °C (S2), which suggests that the grains are loosely connected at low annealing temperatures. The T_{MI} is an extrinsic property that strongly depends on the synthesis conditions and microstructure (e.g. grain boundary density) [4].

The MR as a function of field for various temperatures is shown in Fig. 2. The MR of the LCMO samples having average grain sizes of 16–73 nm not only increases as the grain size decreases but also does as the magnetic field increases. It can be observed that at $T = 30$ K, LFMR (at $H = 3$ kOe) is about 22%, 21%, 19%, 17% and 16% for the 16 nm, 21 nm, 35 nm, 43 nm and 73 nm samples, respectively. Except for a few less evident dependence (low temperature curves of S3 and high temperature curves of S6), all the other observed LFMR(H) show a clear decrease of the magnetoresistance with increasing temperature. The MR in the polycrystalline sample is dominated by transport across grain boundaries field and is extremely sensitive to an applied magnetic field. A steady increase of MR as approaching T_C , resulting from the intrinsic contribution MR_{int} was observed in an high magnetic field as reported by other authors [3,14].

In order to explain the magnetic field dependence of magnetoresistance in granular LCMO we used a phenomenological model which takes into account the spin-polarized tunneling at the grain boundaries [14,17]. The intrinsic contribution to the magnetoresistance is separated from the contribution coming from intergranular spin-polarized transport with paying attention to the domain wall motion across the grain boundaries in an applied magnetic field. According to this model we get the expression for MR as:

$$MR = -A' \int_0^H f(k) dk - JH - KH^3 \quad (1)$$

Within the approximation of the model, in zero field the domain walls are pinned at the grain boundaries pinning centers with pinning strengths k . The grain boundaries have a distribution of pinning strengths (defined as the minimum field needed to overcome a particular pinning barrier) given by $f(k)$, expressed as:

$$f(k) = A \exp(-Bk^2) + Ck^2 \exp(-Dk^2) \quad (2)$$

All the adjustable fitting parameters, A , B , C , D , J , K with A' absorbed in A and C , determined from a nonlinear least square fitting to calculate MR_{spt} , which defined as:

$$MR_{spt} = - \int_0^H f(k) dk \quad (3)$$

Differentiating Eq. (1) with respect to H and putting into Eq. (2), we get:

$$\frac{d(MR)}{dH} = A \exp(-BH^2) + CH^2 \exp(-DH^2) - J - 3kH^2 \quad (4)$$

The experimental MR- H curves were differentiated and fitted to Eq. (4) to find the best-fit parameters at several temperatures. Fig. 3(a-c) shows the differentiated curves and the best-fit functions at $T = 30$ K for S3, S5 and S7 samples. Using the best-fit param-

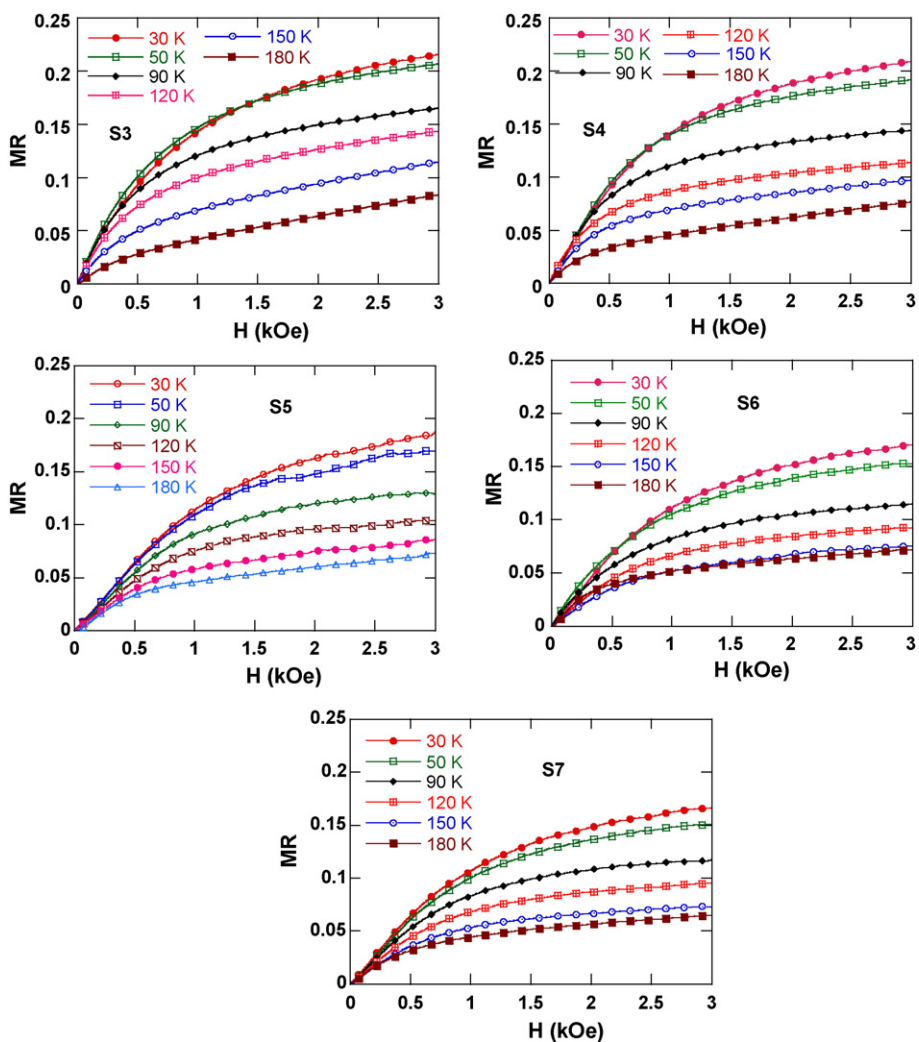


Fig. 2. MR as a function of magnetic field for LCMO samples at several temperatures.

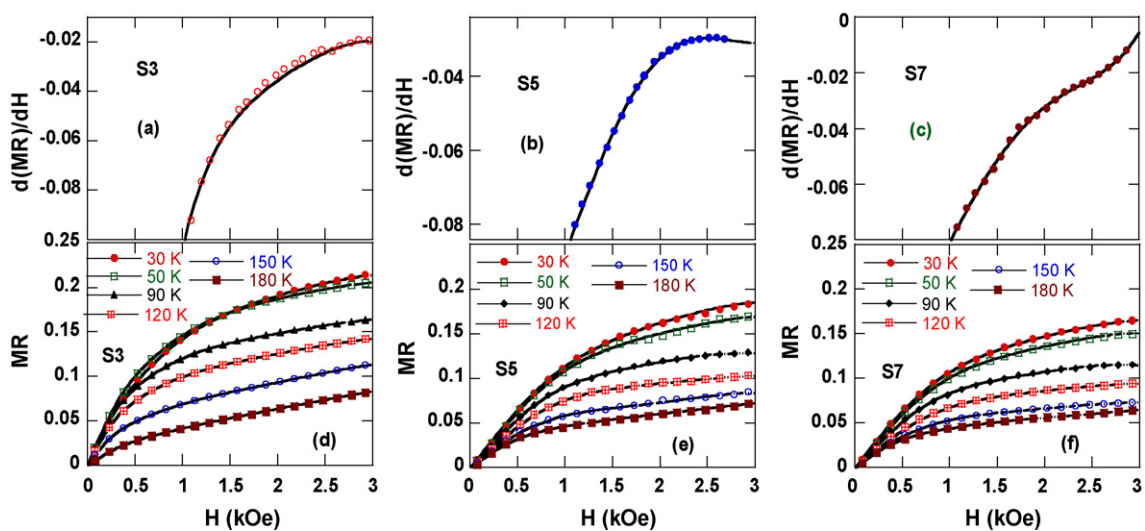


Fig. 3. (a–c) The derivative of the experimental (MR–H) curve (dots) and the fitted curve (lines) using Eq. (4) at 30 K and (d–f) experimental (MR–H) curve (dots) and the fitted curve (lines) using Eq. (1) at various temperatures for samples S3, S5, S7.

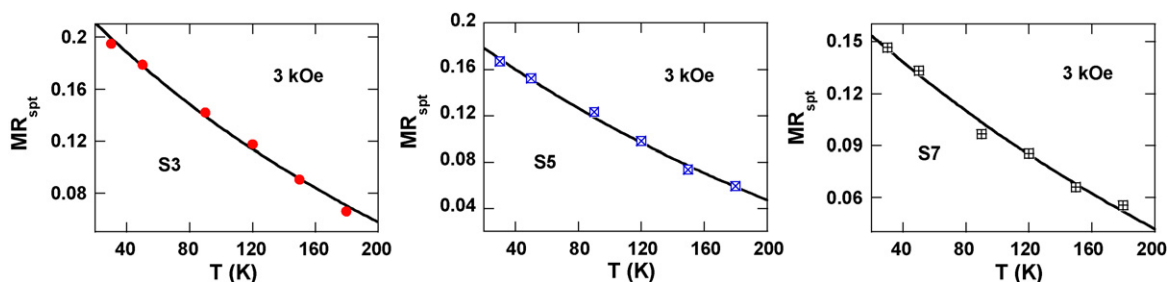


Fig. 4. Temperature dependence of MR_{spt} for S3, S5 and S7 at 3 kOe: the dots are the experimental points and the line is the fitted curve. The best fit of MR_{spt} to a function of form $a + b/(c + T)$.

Table 1

The obtained fitting parameters for $\text{La}_{0.7}\text{Ca}_{0.3}\text{MnO}_3$ (S3, S5, S7), $\text{La}_{2/3}\text{Sr}_{1/3}\text{MnO}_3$ [2] and $\text{La}_{0.55}\text{Ho}_{0.15}\text{Sr}_{0.3}\text{MnO}_3$ [14] with the expression of the type $a + b/(c + T)$.

	S3	S5	S7	[2]	[13]
a	-0.34386	-0.35409	-0.3639	-0.10	-0.3468
b (K)	261.88	293.51	339.79	129	238.5
c (K)	451.95	530.93	633.0	255	446.5

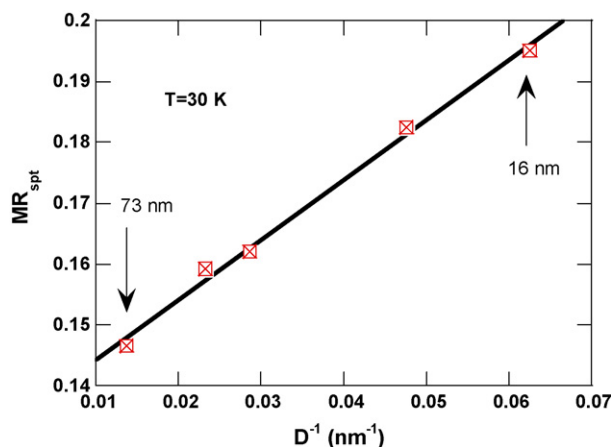


Fig. 5. MR_{spt} versus the surface/volume ratio of the samples with the different grain size at 30 K.

eters we fitted Eq. (1) to our experimental $MR-H$ curves at several temperatures. Fig. 3(d–f) shows excellent fit for the experimental curves to Eq. (1) for samples at several temperatures below T_{MI} .

Hwang et al. [2] observed earlier that the temperature dependence of MR_{spt} is described quite well by an expression of the type $a + b/(c + T)$, which is characteristic of spin-polarized tunneling in granular ferromagnetic systems. Our fitted results for $MR_{\text{spt}}(T)$ as a function of form $a + b/(c + T)$ is shown in Fig. 4. The fitted curve matches well with the extracted values of MR_{spt} and the fitting parameter c increases monotonically when increasing the grain size. However, our values of b and c for the best fit are much higher compared to that reported in [2,14] although the T_{C} of our system is much smaller (see Table 1). The intergranular spin-polarized tunneling has different temperature dependences for ferromagnetically and superparamagnetically coupled grains [18].

Fig. 5 shows the enhanced grain surface effect on MR_{spt} for the five samples (16–73 nm) at 30 K. We also obtained a linear relationship between MR_{spt} and the surface/volume ratio of the grains. It seems that higher values of MR_{spt} and hence MR at low temperature could be attained by diminishing further the grain size.

4. Conclusions

In summary, we have shown that the low-field magnetoresistance of ceramic $\text{La}_{0.7}\text{Ca}_{0.3}\text{MnO}_3$ clearly depends on the grain size.

The low-field magnetoresistance increases as decreasing the grain size. This increase probably arises from spin-polarized transport at the grain boundaries. The phenomenological model used for separating out the MR arising from spin-polarized transport from the intrinsic contribution in our nanosize LCMO samples, fits quite well with the experimental data for the magnetic field and temperature dependence of magnetoresistance on LCMO samples. We have also shown that interfaces and surface effects play a crucial role in magnetic, electronic transport and magneto transport behavior of the nanosize samples. Enhancement of the surface magnetic disorder may result in the low-field magnetoresistance response. The reactive milling method appears to be an effective method to prepare manganite samples for this attractive approach.

Acknowledgments

This work was supported financially by NAFOSTED (CODE: 103.02.48.09). The authors are thankful to the IMS National Key Laboratory for Electronic Materials and Devices and Nha Trang Pedagogic College.

References

- [1] C. Zener, Phys. Rev. 82 (1951) 403.
- [2] H.Y. Hwang, S.W. Cheong, N.P. Ong, B. Batlogg, Phys. Rev. Lett. 77 (1996) 2041–2044.
- [3] P. Dey, T.K. Nath, Phys. Rev. B 73 (2006) 214425.
- [4] P.K. Siwach, U.K. Goutam, P. Srivastava, H.K. Singh, R.S. Tiwari, O.N. Srivastava, J. Phys. D: Appl. Phys. 39 (2006) 14–20.
- [5] L.L. Balcells, J. Fontcuberta, B. Martínez, X. Obradors, Phys. D: Condens. Matter 10 (1998) 1883–1890.
- [6] L.E. Hueso, F. Rivadulla, R.D. Sánchez, D. Caerio, C. Jardón, C. Vázquez-Vázquez, J. Rivas, M.A. Lopez-Quintela, J. Magn. Magn. Mater. 189 (1998) 321–328.
- [7] M.A. Lopez-Quintela, L.E. Hueso, J. Rivas, F. Rivadulla, Nanotechnology 14 (2003) 212–219.
- [8] A. Gaur, G.D. Varma, H.K. Singh, J. Phys. D: Appl. Phys. 39 (2006) 3531–3535.
- [9] L.W. Lei, Z.Y. Fu, J.Y. Zhang, H. Wang, Mater. Sci. Eng. B 128 (2006) 70–74.
- [10] P.T. Phong, N.V. Khiem, N.V. Dai, D.H. Manh, L.V. Hong, N.X. Phuc, Mater. Lett. 63 (2009) 353–356.
- [11] J. Kumar, R.K. Singh, P.K. Siwach, H.K. Singh, R. Singh, O.N. Srivastava, J. Magn. Magn. Mater. 299 (2006) 155–160.
- [12] A. Gaur, G.D. Varma, Solid State Commun. 144 (2007) 138–143.
- [13] P.K. Siwach, R. Prasad, A. Gaur, H.K. Singh, G.D. Varma, O.N. Srivastava, J. Alloys Compd. 443 (2007) 26–31.
- [14] P. Raychaudhuri, T.K. Nath, A.K. Nigam, R. Pinto, J. Appl. Phys. 84 (1998) 2048–2052.
- [15] D.H. Manh, N.C. Thuan, P.T. Phong, L.V. Hong, N.X. Phuc, J. Alloys Compd. 479 (2009) 828–831.
- [16] D.H. Manh, P.T. Phong, T.D. Thanh, L.V. Hong, N.X. Phuc, J. Alloys Compd. 491 (2009) 8–12.
- [17] P.T. Phong, N.V. Khiem, N.V. Dai, D.H. Manh, L.V. Hong, N.X. Phuc, J. Alloys Compd. 484 (2009) 12–16.
- [18] J.S. Helman, B. Abeles, Phys. Rev. Lett. 37 (1976) 1429–1432.
- [19] A. Tiwari, K.P. Rajeev, Phys. Rev. B 60 (1999) 10591–10593.
- [20] Neeraj Panwar, V. Sen, D.K. Pandya, S.K. Agarwal, Mater. Lett. 61 (2007) 4879–4883.
- [21] G. Venkataiah, J.C.A. Huang, P.V. Reddy, J. Magn. Magn. Mater. 322 (2010) 417–423.